Feiyue Zhou ¹ ; Shuze Ma ¹ ; Lei Li ¹ ; Jiale Zhang ¹ ; Chunlei Xiao ¹ ; Wenrui Dong ¹ ; Hongwei Li ■ ¹



J. Chem. Phys. 162, 094201 (2025) https://doi.org/10.1063/5.0249941





Articles You May Be Interested In

KoopmanLab: Machine learning for solving complex physics equations

APL Mach. Learn. (September 2023)

Experimental realization of a quantum classification: Bell state measurement via machine learning

APL Mach. Learn. (September 2023)







A new apparatus for gas-phase low temperature kinetics study: Kinetics measurement and product detection of the CH + propene reaction at 23 K

Cite as: J. Chem. Phys. 162, 094201 (2025); doi: 10.1063/5.0249941 Submitted: 21 November 2024 • Accepted: 13 February 2025 • Published Online: 4 March 2025







Feiyue Zhou,^{1,2} D Shuze Ma,^{1,2} Lei Li,¹ D Jiale Zhang,¹ Chunlei Xiao,^{1,2} Wenrui Dong,^{1,2} and Hongwei Li^{1,2,a}

AFFILIATIONS

- ¹ State Key Laboratory of Molecular Reaction Dynamics and Dalian Coherent Light Source, Dalian Institute of Chemical Physics, Chinese Academy of Sciences, Dalian, Liaoning 116023, China
- ²University of Chinese Academy of Sciences, Beijing 100049, China

ABSTRACT

We have developed a novel instrument to study reaction kinetics of astrochemical interest at low temperatures. This setup integrates laser-induced fluorescence (LIF) and vacuum ultraviolet (VUV) photoionization reflectron time-of-flight mass spectrometry (ReTOFMS) with a supersonic uniform low-temperature flow. A pulsed helium Laval nozzle with a Mach number of 6 was employed, achieving a temperature of 23 \pm 3 K and a density of (2.0 \pm 0.4) \times 10¹⁶ molecule cm⁻³. The second-order rate coefficient for the reaction between the methylidyne radical (CH) and propene (C₃H₆) at 23(3) K was determined to be (3.4 \pm 0.6) \times 10⁻¹⁰ cm³ molecule⁻¹ s⁻¹ using LIF kinetics measurements. VUV (118.27 nm) photoionization ReTOFMS detected a dominant product channel, CH + C₃H₆ \rightarrow C₄H₆ + H, without isomer identification. Another less intense mass peak at m/z 53 was also observed, which could either result from the dissociative ionization of the energized C₄H₆ primary products or indicate another product channel, C₄H₅ + H₂. Given the presence of CH and C₃H₆ in cold molecular clouds (e.g., TMC-1, Lupus-1a, L1495B, L1521F, and Serpens South 1a), it is predicted that these products can exist in low-temperature interstellar environments.

Published under an exclusive license by AIP Publishing. https://doi.org/10.1063/5.0249941

I. INTRODUCTION

Low-temperature gas phase kinetics are crucial for developing accurate astrochemical models that enhance our understanding of chemical evolution in cold molecular clouds, the interstellar medium (ISM), and planetary atmospheres. As of September 2024, over 320 molecules, including more than 50 hydrocarbons, have been identified in the ISM or circumstellar shells. ^{1,2} Polycyclic aromatic hydrocarbons (PAHs) are of particular interest, as they likely contribute to the unidentified infrared emission bands observed throughout the universe. ^{3,4} Consequently, understanding the chemical processes that produce longer carbon chains, aromatic molecules, and ultimately PAHs is increasingly important in low-temperature environments. Numerous chemical networks have been developed to replicate observed abundances of these interstellar species. ^{5–9}

However, in the absence of experimental low-temperature kinetics data, reaction rate coefficients are often extrapolated from high-temperature data, which can be problematic for reactions deviating from Arrhenius behavior. Due to quantum effects, the rate coefficient for such reactions can increase significantly as temperature decreases. ^{10–13} Therefore, experimental studies on low-temperature kinetics—including reaction rate coefficients and product branching ratios (BRs)—are essential for astrochemical modeling and serve as benchmarks for theoretical studies. The methylidyne radical (CH), a highly reactive species, plays a crucial role in synthesizing larger hydrocarbons and complex organic interstellar molecules. Although the reaction kinetics and product formation from the reaction between CH and propene (both species have been detected in dark molecular clouds) have been studied at room temperature, they remain unexplored at low temperatures.

a) Author to whom correspondence should be addressed: lihw@dicp.ac.cn

A *de Laval* nozzle has an axisymmetric convergent–divergent profile that accelerates high-pressure gas to supersonic speeds through isentropic expansion. This process converts the thermal energy of the gas into kinetic energy, producing a uniform supersonic flow characterized by a high Mach number, low temperature, and relatively high number density (10¹⁶–10¹⁷ molecule cm⁻³) within the isentropic core along the flow axis. ^{14,15} This approach overcomes issues seen in traditional cryogenic cooling, where reactant molecules condense on chamber walls at low temperatures. In the 1980s, Rowe and colleagues pioneered the CRESU (Cinétique de Réaction en Ecoulement Supersonique Uniforme) technique, which uses a Laval nozzle in gas-phase ion-molecule reaction kinetic studies at temperatures as low as 20 K, with detection by quadrupole mass spectrometry. ^{16,17} In initial experiments, ions were generated by electron impact on the gas in the flow, and later advancements introduced mass-selective capabilities for the ions. ^{18,19}

Many radical-neutral reactions in the gas phase remain rapid at low temperatures due to barrierless pathways or quantum effects. The CRESU technique has been widely adopted by several international groups to study the neutral-neutral reaction kinetics using spectroscopic detection methods. 11,20-23 In this setup, radicals are typically produced by pulsed laser photolysis (PLP) along the flow axis, and the time-dependent concentration profile of reactants (or products) is monitored via laser-inducedfluorescence (LIF), 10,15,20,24,25 chemiluminescence, 13,26 and resonance fluorescence. ^{27,28} These detection methods are highly sensitive and selective for small species but lack the capability to probe larger, complex molecules. Suits and colleagues employed chirped-pulse Fourier-transform microwave spectroscopy (CP-FTMW) as a nearly universal probe in pulsed Laval uniform flow experiments. ^{29,30} This microwave spectroscopy technique, with its wide frequency range, provides isomer and conformer-specific, quantitative simultaneous detection of multiple reaction products and intermediates.^{29,31} CP-FTMW probes the free induction decay of rotational coherence, which is unfortunately attenuated by high collision frequency in the dense Laval flow. Recent efforts have improved detection sensitivity under lower-pressure conditions by using airfoil-shaped sampling in the flow³² or secondary expansion following an extended Laval nozzle.33 Infrared absorption spectroscopy has also been coupled with uniform Laval flow experiments using single-frequency lasers³⁴ and broadband light sources.^{36,37} The extended interaction path length between the light and sample achieved by cavity-enhanced techniques is desired to increase sensitivity for detecting trace species during reactions.

Universal detection using vacuum ultraviolet (VUV) photoionization time-of-flight mass spectrometry was first introduced by Leone and colleagues for studying neutral-neutral reaction kinetics in Laval uniform flows. This technique has since been adopted by other groups for fundamental studies on gas-phase nucleation, cluster formation, and soot formation at low temperatures. A skimmer samples the isentropic core of the uniform flow and supports differential pumping to maintain the high vacuum required for mass spectrometry. Concerns arose regarding flow uniformity disturbances from shock waves created by the skimmer mounting surface; thus, airfoil sampling were designed to minimize such effects. The photoionization light source has also been upgraded to tunable VUV synchrotron radiation, enabling soft

ionization to identify isomer-specific reaction products.^{44,45} This advancement has been successfully demonstrated in kinetics studies of reactions between C₂H and ethene, propene, and butene isomers at 79 K, where isomer-resolved products were identified, and their branching ratios and overall bimolecular reaction rate coefficients were measured.^{46,47} To our knowledge, only stable products, not radicals, have been detected in bimolecular reactions in the uniform supersonic flow experiment using mass spectroscopy.

In this study, we present a new instrument for studying radical-neutral reaction kinetics of astrochemical interest, which combines LIF and VUV (118.27 nm) photoionization reflectron time-of-flight mass spectrometry (ReTOFMS) detection with lowtemperature supersonic uniform flow generated by a pulsed Laval nozzle. PLP-LIF detection monitors the radical's temporal profile during the reaction, allowing for determination of the reaction rate coefficient, while ReTOFMS detects reaction products and intermediates. The reaction between CH and propene has been studied by several groups, with reaction rate coefficients measured from 77 to 298 K and product branching ratios determined only at 298 K. 48-51 The reaction mechanism has also been theoretically explored with different levels of theory, showing CH addition or insertion to propene followed by complex isomerization and decomposition pathways. 52-54 At room temperature, 1,3-butadiene is the primary product channel,⁵⁰ which has been seen as a precursor to synthesize the simplest aromatic hydrocarbon, benzene. 55 However, no experimental characterization of reaction products at low temperatures has been reported. Here we present the design of our new experimental setup, characterization of the uniform supersonic flow, measurements of the reaction rate coefficient, and product detection for the CH + C₃H₆ reaction at 23 K.

II. EXPERIMENTAL METHODS

A. Laval flow chamber design

The new experimental apparatus consists of a pulsed lowtemperature uniform (Laval) flow chamber, LIF detection, and a ReTOFMS detection chamber. As shown in Fig. 1, the uniform flow molecular source is housed in a cylindrical vacuum chamber (1.8 m in length, 0.5 m in diameter), evacuated by a mechanical booster pump (Edwards EH2600) backed by two dry multistage Roots pumps (Edwards nXR60i and nXL200i). Slip gas is introduced to maintain a vacuum between 0.1 and 1.0 Torr, depending on flow conditions. A helium Laval nozzle was designed and utilized here to generate a supersonic uniform flow with a Mach number of 6. Based on the pulsed-flow design by the Suits group, a high-throughput homemade pulsed valve driven by a piezoelectric stack actuator (Coremorrow PSt 150) is coupled to the Laval nozzle, reducing the gas load and pump capacity requirements compared to continuousflow designs. The pulsed Laval nozzle operates at a 5 Hz repetition rate with a 7.6 ms pulse duration. Two fast pressure transducers (Kulite XTL-190), located in the reservoir and downstream of the post-nozzle flow, monitor the flow pressure to achieve the required conditions. Capacitance diaphragm gauges (INFICON CDG025D) measure the source chamber pressure and calibrate the pressure transducers. The entire pulsed Laval nozzle assembly is mounted on a linear translation stage with a 60 cm travel distance inside the source chamber, allowing precise remote adjustments during flow characterization.

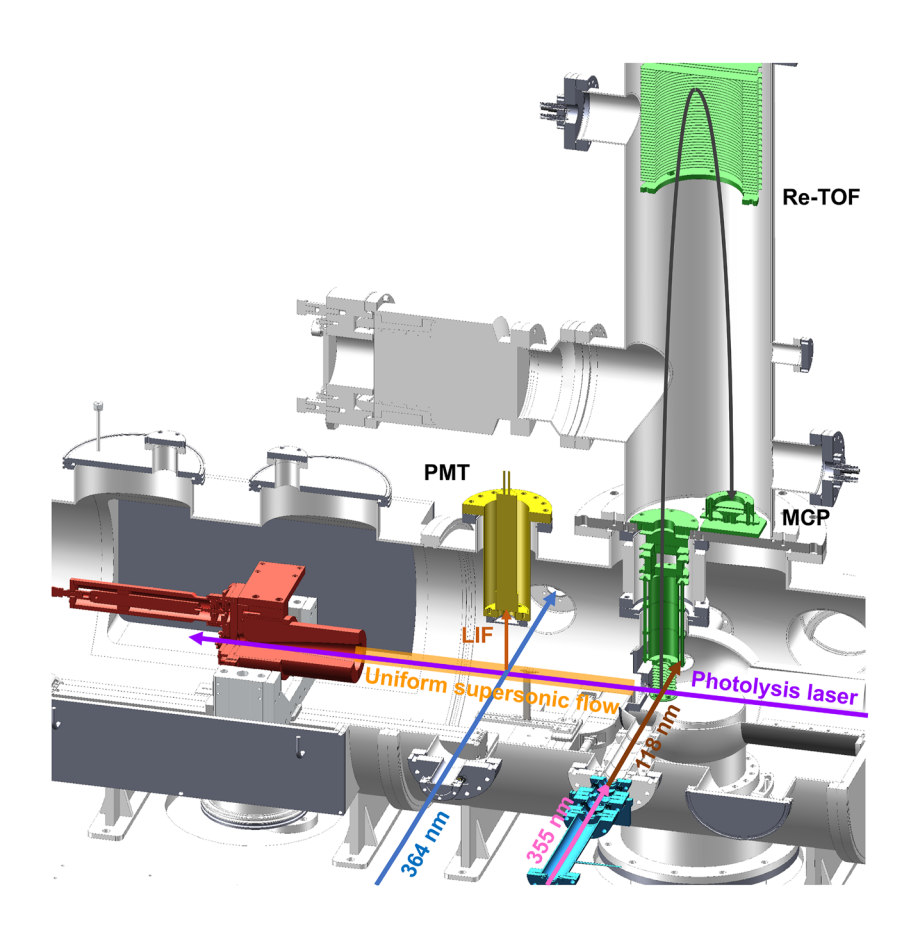


FIG. 1. Apparatus: The schematic used for the low-temperature kinetics study. The setup highlights the pulsed Laval nozzle assembly (red), uniform supersonic flow (orange), PMT detection (yellow), VUV tripling cell (blue), ReTOFMS detection (green), and lasers labeled with their corresponding wavelengths.

B. Radical generation and LIF detection

The CH radical is generated coaxially within the uniform supersonic flow via multiphoton photolysis of CHBr3 at 248 nm. The precursor, CHBr3 (Sigma-Aldrich, 99%), is vaporized using a homemade vaporizer and mixed with C₃H₆ (Dalian Special Gases Co., LTD., 99.5%) and helium carrier gas. The uniform supersonic flow has typical densities of CHBr₃: $\sim 7.5 \times 10^{12}$ molecule cm⁻³, C₃H₆: $(1.5-14) \times 10^{13}$ molecule cm⁻³, with the He carrier gas balancing to a total density of 2.0×10^{16} molecule cm⁻³. All gas flows are controlled by mass flow controllers (MKS, GM50 series). The 248 nm radiation from an excimer laser (Coherent COMPex 205, photon flux 90 mJ cm⁻²) is equipped with unstable resonators to improve the collimation of the output laser beam and is counter-propagated through the uniform flow. Using the same CH yield of $(5 \pm 2.5) \times 10^{-4}$ from the photolysis of CHBr₃ at 248 nm, as reported by Romanzin et al.,⁵⁶ under a laser fluence of 44 mJ cm⁻² per pulse, the density of CH radical under the flow condition in this work is estimated to be 3.8 × 10⁹ molecule cm⁻³. CH radicals are state-selectively probed using in situ LIF detection, with excitation at the CH $B^2\Sigma^- \leftarrow X^2\Pi$ (1, 0) band around 364 nm and fluorescence via the CH $B^2\Sigma^- \longrightarrow X^2\Pi$ (1, 1) band around 404 nm. The UV radiation around 364 nm for the probe laser is generated by frequency-doubling the output of a Nd:YAG (Beamtech Nimma-900, 532 nm) pumped dye laser (Sirah, Cobra Stretch) utilizing dye LDS 722 (Exciton). The UV radiation is directed perpendicular to the uniform flow, and a fluorescence

collection assembly is positioned above the intersection of photolysis and probe laser. The collection assembly (yellow parts in Fig. 1) consists of a plano-convex lens (150 mm focal length, anti-reflection coated at 404 nm), filter sets (Semrock, FF01-300/LP, FF01-420/10), and a photomultiplier tube (Hamamatsu PMT, R1398). The temporal profile of CH loss due to reaction with propene is monitored by LIF while adjusting the delay time between the photolysis and probe lasers, which allows for the derivation of the overall reaction rate coefficient. At each laser delay time, the CH intensity was collected by averaging its LIF trace 128 times and integrating between 100 and 800 ns. The kinetics trace of the CH loss profile was repeated three times for each propene concentration.

C. ReTOFMS detection

The reactants, intermediates, and products of the reaction in the low-temperature uniform flow are detected by VUV (118.27 nm) photoionization ReTOFMS detection. A 1 mm diameter skimmer (Beam Dynamics, Model 2) samples the isentropic core of the uniform flow, and provides differential pumping from the low vacuum of the Laval flow chamber to the high vacuum condition required for mass spectrometry detection. A streamlined flange, inspired by Durif *et al.*,⁴⁵ was designed to mount the skimmer, minimizing disturbance to the uniform flow caused by the shock wave induced by the skimmer mount. The ion accelerator and detection regions are evacuated by two turbomolecular pumps (Edwards nEXT730,

730 L/s) backed with a dry scroll pump (Edwards XDS35i, 35 m³/h), maintaining the vacuum in the detection region at $\sim 10^{-6}$ Torr during the experiment. A homemade ReTOFMS assembly (green parts shown in Fig. 1) has been designed to couple to Laval flow, and consists of ion accelerator electrodes, an Einzel lens, x axis and y axis deflectors, ion reflector, and a microchannel plate (MCP) detector. A constant voltage of 1200 V is applied to the repeller electrode, while a pulsed voltage of 150 V is applied to the y axis deflector to deflect unwanted ion signals, specifically the overwhelming C₃H₆ signal in the present work. The VUV photoionization interaction region is located 5 cm from the skimmer tip. The VUV radiation at 118.27 nm is generated by tripling the third harmonic output of 355 nm radiation from a Nd:YAG laser (Beamtech Optronic Nimma-900) in a xenon cell. The ions are then extracted and accelerated in ReTOFMS and detected by a Z-stack MCP detector. These signals were amplified by a preamplifier (Femto, DHPCA-100) and recorded by an ADC card (FCFR-USB9982C). The resolution of the mass spectra (m/\Delta m) was estimated to be around 1000. Synchronization and timings of all components, including the pulsed valve, lasers, and detection instruments, are controlled by a delay generator (Quantum Composers 9528).

III. RESULTS AND DISCUSSION

A. Uniform flow characterization

A helium Laval nozzle with a Mach number of 6 was employed in this study, 34,57 and the properties of its post-nozzle uniform supersonic flow were characterized through Pitot impact pressure measurements. One pressure transducer was placed in the reservoir to monitor reservoir pressure (P_0), while another was positioned in a Pitot tube facing the flow to measure the impact pressure (P_i). For isentropic flow, the Mach number (M)—defined as the flow velocity divided by the local speed of sound—is related to P_0 and P_i , as derived from the Rayleigh formula, 58 shown in Eq. (E1). Here, $\gamma = C_p/C_v = 1.667$ represents the heat capacity ratio for the helium carrier gas,

$$\frac{P_i}{P_0} = \left(\frac{(\gamma+1)M^2}{(\gamma-1)M^2+2}\right)^{\frac{\gamma}{\gamma-1}} \left(\frac{\gamma+1}{2\gamma M^2-\gamma+1}\right)^{\frac{1}{\gamma-1}}.$$
 (E1)

A trial value of M is determined iteratively to match the measured value of P_i/P_0 at various positions in the post-nozzle flow. Subsequently, the temperature (T), pressure (P), and density (ρ) of the post-nozzle flow can be calculated from M using the following equations:

$$\frac{T}{T_0} = \left[1 + \left(\frac{\gamma - 1}{2}\right)M^2\right]^{-1},$$
 (E2)

$$\frac{P}{P_0} = \left[1 + \left(\frac{\gamma - 1}{2}\right)M^2\right]^{\frac{-\gamma}{\gamma - 1}},$$
 (E3)

$$\frac{\rho}{\rho_0} = \left[1 + \left(\frac{\gamma - 1}{2}\right)M^2\right]^{\frac{-1}{\gamma - 1}},$$
 (E4)

where T_0 and ρ_0 represent temperature and density in the reservoir region. ⁵⁸ Optimal flow conditions are achieved by adjusting the reservoir and flow chamber pressures. The reservoir pressure is controlled by pulsed valve timing and gas flow rate, while the flow chamber pressure is regulated by adding slip gas flow into the chamber and partially closing the vacuum pump gate. Both the pulsed Laval nozzle (red part in Fig. 1) and the Pitot tube assemblies are mounted on linear translational stages with travel distances of 60 and 20 cm, respectively. This setup allows for two-dimensional (2D) translation of the Pitot tube relative to the Laval nozzle, providing a comprehensive 2D view of the experimental flow conditions. The optimal flow conditions of this helium Laval nozzle were achieved by setting the reservoir pressure to 39 mbar and the chamber pressure to 0.16 mbar, generating a uniform flow length of 400 mm. Figure 2(a) displays the contour map of density with a radial distance of 13 mm and an axial distance of 400 mm, and Fig. 2(b) illustrates the flow temperature (23 \pm 3 K) and density $([2.0 \pm 0.4] \times 10^{16} \text{ molecule cm}^{-3})$ along the axis of the post-nozzle supersonic flow, as indicated by the black line in Fig. 2(a). The flow velocity was measured to be 1696 ± 10 m/s, and the 400 mm length of the uniform flow corresponds to a maximum reaction time of ~230 μ s under the current flow conditions.

The low-temperature Laval supersonic uniform flow creates a thermal environment that cools the rotational temperature of the species within the flow. Our previous research, along with other studies in the CRESU community, has demonstrated that the rotational temperature correlates with results from the Pitot impact pressure measurement. ^{20,59} The CH ($X^2\Pi$, v = 0) radical in a specific rotational state was detected by exciting it using the CH $B^2\Sigma^ \leftarrow X^2\Pi$ (1, 0) band and collecting fluorescence emitted from the CH $B^2\Sigma^- \to X^2\Pi$ (1, 1) band. The population of the rotational states can be measured by tuning the wavelengths of the probe laser. Because the multiphoton photolysis of CHBr₃ generates CH with internal excitation, it takes a few microseconds for relaxation under flow conditions;⁵⁹ therefore, the CH rotational state distribution was measured with a photolysis-probe delay time of 30 μ s. The rotational temperature was simulated to be 27.2 \pm 0.5 K using the PGOPHER program⁶⁰ with known parameters for both the $X^2\Pi$, v = 0 and $B^2\Sigma^-$, v = 1 states.⁶¹ A good agreement is observed between the rotational state distributions from both experimental and PGOPHER simulation results, with the highest population in the lowest rotational level, as shown in Fig. 2.

B. CH + propene reaction kinetics measured with LIF

The temporal evolution measurements of the CH radical, detected using the PLP-LIF technique, have been widely employed to determine reaction rate coefficients in Laval low-temperature experiments. The temporal profile of the CH radical in the lowest rotational level ($X^2\Pi$, v=0, N=1, J=1.5) shows a rapid rise followed by a slower exponential decay, as shown in Fig. 3(a). The rise corresponds to the relaxation of the CH radical from higher rotational levels upon colliding with helium carrier gas under low-temperature supersonic flow conditions. ⁵⁹ This relaxation process is rapid, allowing the CH radical to reach its lowest rotational level and approach a maximum plateau within 10 μ s, consistent with previous studies. ⁵⁹ The exponential decay of the CH radical's temporal evolution results

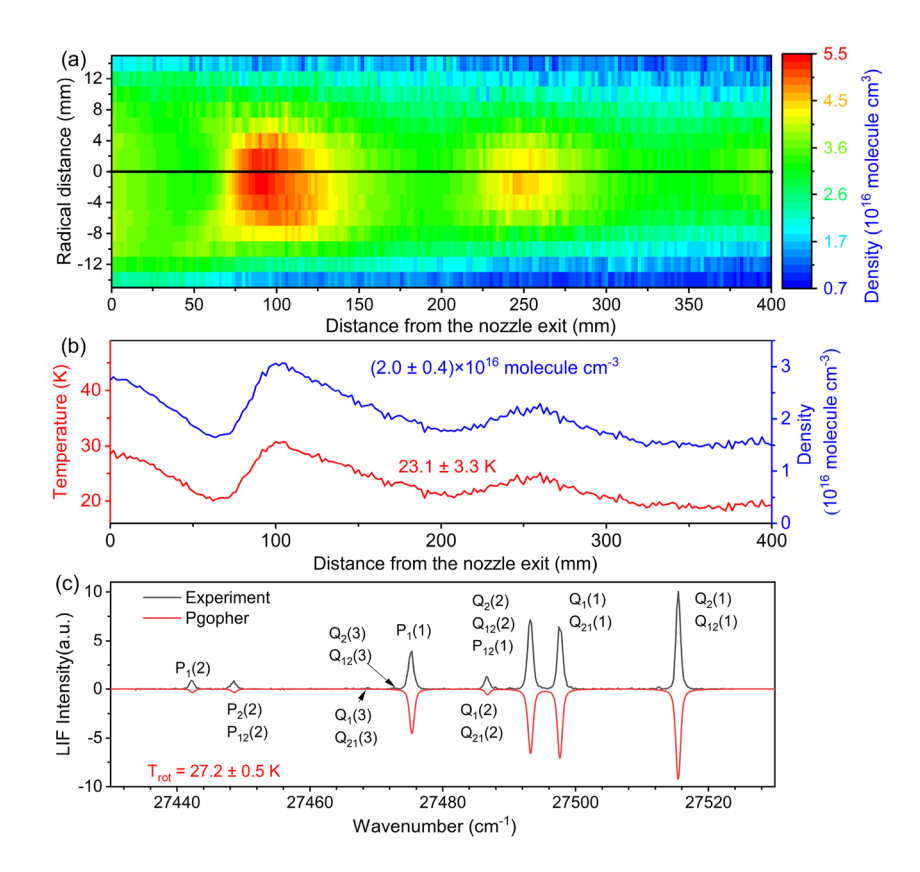


FIG. 2. (a) Density contour map of the uniform supersonic flow from the helium Laval nozzle. (b) Temperature and density profiles along the flow axis obtained from the Pitot measurements. (c) Comparison of the experimental (black) and PGOPHER simulation (red) data on the CH ($X^2\Pi$, $\nu=0$) rotational state distribution

from its reaction with propene, CHBr $_3$ precursor, or other impurities (such as 2-methyl-2-butene, a stabilizer in the CHBr $_3$ sample, 60–120 ppm), as well as diffusion out of the detection region. This is described by the following equation:

$$[CH]_{t} = [CH]_{0} \cdot \exp \{-(k_{2}[C_{3}H_{6}] + k_{other}) \cdot t\}$$

= $[CH]_{0} \cdot \exp (-k_{1st} \cdot t),$ (E5)

where [CH]_t and [CH]₀ are the instantaneous and initial concentrations of the CH radical, respectively, k_2 is the bimolecular reaction rate coefficient for the reaction CH + $C_3H_6 \rightarrow \text{products}$, k_{other} accounts for CH reaction with other molecules and diffusion processes, and k_{1st} is the pseudo-first-order rate coefficient for a given concentration of propene. The temporal evolution of the CH LIF signal occurs under pseudo-first-order conditions, where [C₃H₆] $\sim 10^{13}$ molecule cm⁻³ \gg [CH] $\sim 10^{10}$ molecule cm⁻³, leading to an exponential decay process with a decay rate coefficient given by $k_{1st} = k_2[C_3H_6] + k_{other}$. Furthermore, careful analysis indicates that the experimental LIF signal in the decay region (after 30 μ s) is unaffected by its relaxation process; thus, the LIF signal is fitted using (E5) for times longer than 30 µs. An increase in C₃H₆ concentration results in a faster decay in [CH]_t, as illustrated in Fig. 3(a). Plotting k_{1st} against various C₃H₆ concentrations yields a linear relationship, with its slope representing the second-order reaction rate coefficient for the CH + C_3H_6 reaction, as shown in Fig. 3(b). Using this PLP-LIF pseudo-first-order method, the reaction rate coefficient for the CH + C_3H_6 reaction at 23(3) K was measured to be (3.4 \pm 0.6) \times 10⁻¹⁰ cm³ molecule⁻¹ s⁻¹.

C. ReTOFMS characterization for validation

We have coupled VUV (118.27 nm) photoionization ReTOFMS with Laval uniform supersonic flow to detect the products of low-temperature reactions. Several aspects must be carefully addressed to validate the kinetics measurements with ReTOFMS. First, a 1 mm skimmer mounted on a streamlined flange samples the isentropic core of the uniform flow. The repeated CH rotational distribution measurements in Fig. 2(c), taken just before the skimmer tip, indicate negligible perturbation effects on the flow uniformity caused by the shock wave induced by the skimmer assembly. Second, the linear calibration curve for our ReTOFMS was verified using propene molecules. Propene at various concentrations was introduced into our mass spectrometer via the Laval nozzle, resulting in a linear fit between the mass signal and propene concentration, with $R^2 = 0.9998$, as shown in Fig. S1. This indicates a strong linear MS response associated with the species in the uniform Laval flow. Third, we compared the propene mass signal from skimmer sampling to the pulsed gas profile from the Pitot measurement (shown in Fig. S2). The time-resolved mass response profile is broader than the gas density measured by the Pitot tube. This broadening effect was further characterized by detecting the iodine's temporal evolution using ReTOFMS following the photolysis of CH₃I 248 nm. As shown

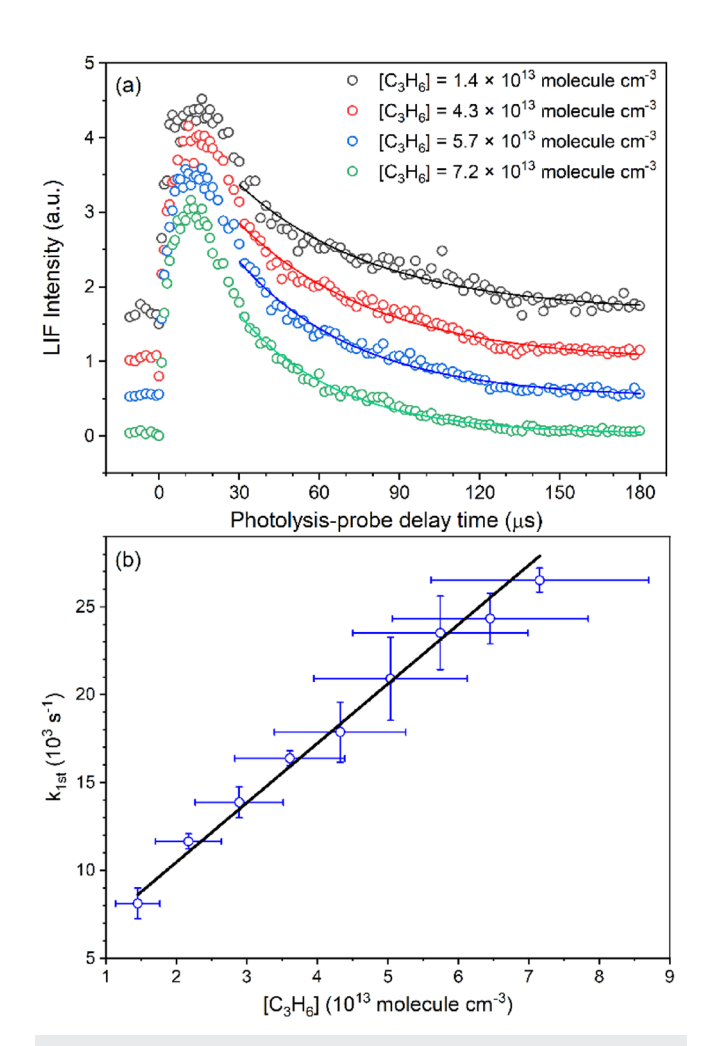


FIG. 3. (a) Representative transient CH integrated fluorescence signal as a function of the delay time between the photolysis and LIF probe lasers at 23(3) K, along with single exponential fits for various C_3H_6 concentrations. (b) Plot of the pseudo-first-order rate vs different C_3H_6 concentrations. The slope of the linear fit determines the second-order rate coefficient, $k_2=(3.4\,\pm\,0.6)\times10^{-10}\,\text{cm}^3$ molecule $^{-1}\,\text{s}^{-1}$ (1 σ level) for the CH $_{+}$ propene reaction at 23(3) K.

in Fig. S3(a), the I temporal profile exhibits a slow formation. However, in the previous UV photodissociation dynamics studies of CH₃I, the product's anisotropic distribution feature indicates that photodissociation is prompt (<1 ns). 62,63 The slower rise of the I temporal profile in the present work is attributed to the velocity spread occurring during transit from the skimmer tip to the photoionization probe region, as discussed by Taatjes⁶⁴ and recently by Gurusinghe *et al.* 32 A Gaussian-shaped system response function is introduced here to compensate for this and enable valid time-resolved mass spectroscopy measurements, inspired by Bouwman *et al.* 47 If we consider a unit yield following the photolysis of CH₃I, a step function, as shown in Fig. S3(b), is used here as the original function. A Gaussian profile with a Full-Width-at-Half-Maximum (FWHM) of 12 μ s and unit area [shown in Fig. S3(c)] accounts for the response function of our time-resolved ReTOFMS in the He

supersonic uniform flow at 23(3) K. Since the assumed step function is an ideal case for a photodissociation process, the 12 μ s FWHM Gaussian profile is likely to be overestimated.

D. Product detection using ReTOFMS

A careful search using 118.27 nm photoionization ReTOFMS was conducted to identify products from the CH + propene reaction. Figure 4 displays the mass spectrum (average over 150 shots for each trace) with mass-to-charge ratios (m/z) of 53, 54, and 55 detected in the presence of both CHBr₃ and propene molecules, along with the 248 nm photolysis laser present. The mass peaks of m/z 53 and 54 were not observable without either CHBr₃, propene, or the photolysis laser. Some background signal was seen at m/z 55 with only propene present in the uniform flow, likely due to VUV photolysis or VUV-induced reactions of impurity molecules, and this signal will be subtracted in further analysis. To determine whether these mass peaks m/z 53, 54, and 55 (C₄H₅, C₄H₆, and C₄H₇) originate from the CH + propene reaction, their temporal evolution profiles were measured over different reaction times. The raw TOF traces were averaged 150 times and integrated for each mass at each reaction time to generate their temporal evolution. As shown in Fig. 5(d), the kinetics traces of m/z = 53 and 54 increase with reaction time, reaching a maximum within 50 μ s. Moreover, the rise time and maximum plateau for each mass vary with different propene concentrations, which is a typical pattern for products arising from a reaction. However, the kinetics trace for m/z 55 (after background subtraction) exhibits a decay pattern between 0 and 30 μ s, followed by an increase. The distinct behavior of m/z 55, compared to 53 and 54, indicates that m/z 55 (C₄H₇ cations) does not directly result from the CH + propene reaction.

The dominant mass peak appears at m/z 54 (C₄H₆ cations) and corresponds to CH + $C_3H_6 \rightarrow C_4H_6$ + H reaction channel. Eight C₄H₆ isomers are predicted from the CH + C₃H₆ reaction, as summarized in Table I, based on the comprehensive potential energy surface calculations by Ribeiro and Mebel using the ab initio CCSD(T)-F12/CBS//B3LYP/6-311G(d,p) level of theory.54 All C₄H₆ isomers have ionization energies below 10.48 eV (the photon energy of the present VUV probe)65 and are produced in the overall exothermic reaction, as listed in Table I. Since the single VUV photon energy does not have the capability to resolve isomers, all these C₄H₆ isomers seem to be observable in the present work using 118.27 nm photoionization ReTOFMS. A tunable VUV light source is desired to collect the photoionization efficiency (PIE) spectrum to identify the isomers. Recently, this reaction has been studied in the gas phase at 298 K and 4 Torr using VUV synchrotron photoionization mass spectrometry (PIMS) by Trevitt et al.⁵⁰ In their PIMS study, only the C₄H₆ + H product channel was observed, with C_4H_6 isomers identified as 1,3-butadiene (branching ratio, BR = 0.63 \pm 0.13), 1,2-butadiene (BR = 0.25 \pm 0.05), and 1-butyne (BR = 0.12 \pm 0.03), based on fitting experimental PIE spectra to measured spectra of known C₄H₆ isomers. More recently, the reaction dynamics of this reaction was studied by crossed molecular beams (CMBs) under single-collision conditions by the Kaiser group. 51 The product channel of C₄H₆ + H was also detected by electron impact (80 eV) ionization. In contrast to the detection of 1,3-butadiene, 1,2-butadiene, and 1-butyne isomers in the PIMS experiment under thermal flow conditions, 1-methylcyclopropene and 3-methylcyclopropene were

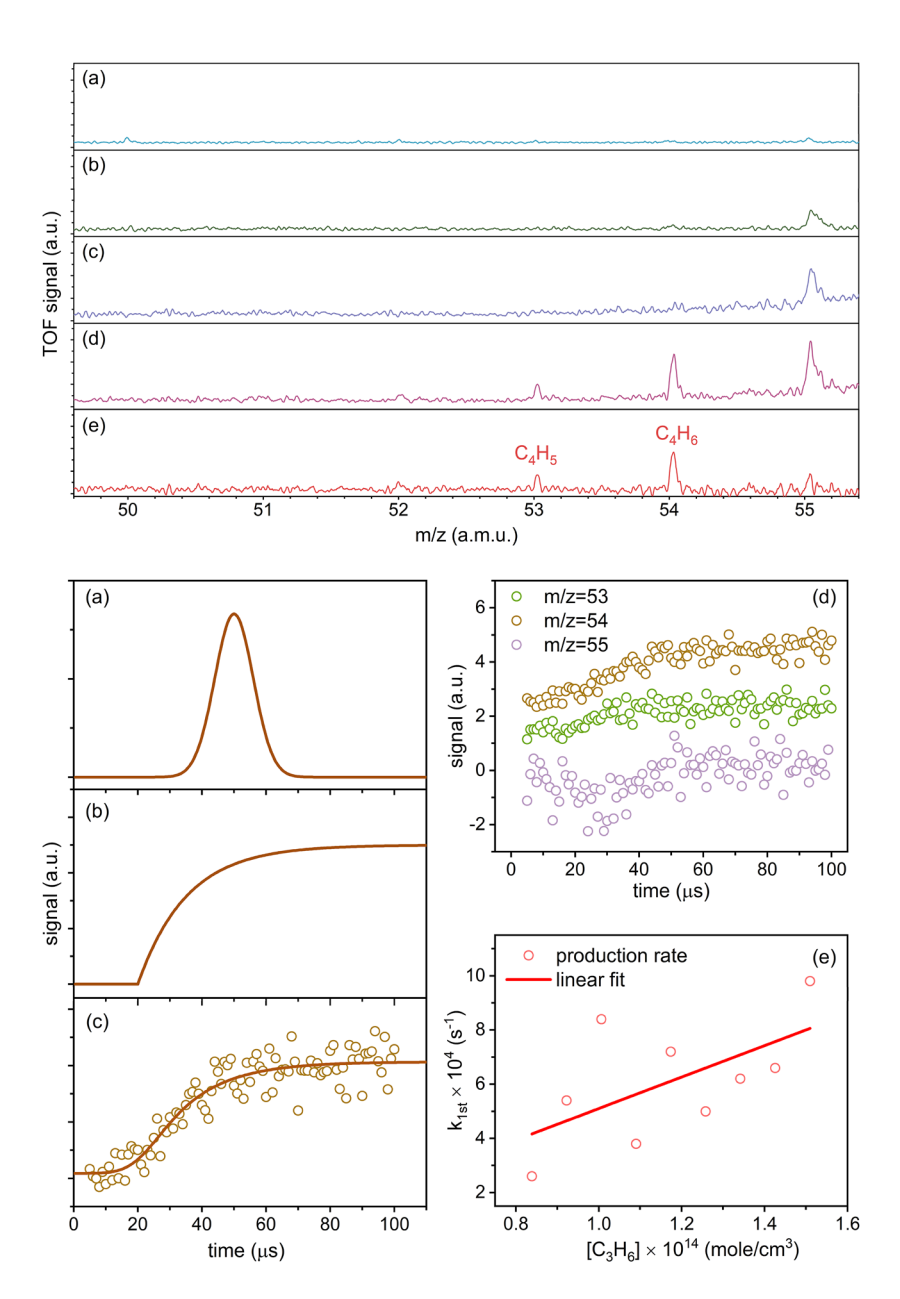


FIG. 4. VUV photoionization mass spectra under different conditions at a kinetic time of 100 μ s. Mass spectrum of (a) only CHBr₃ with photolysis laser on, (b) only C₃H₆ with photolysis laser on, (c) both CHBr₃ and C₃H₆ present with photolysis laser off, (d) both CHBr₃ and C₃H₆ present with photolysis laser on, and (e) subtraction of spectrum (c) from spectrum (d).

FIG. 5. (a) Gaussian shaped $(12-\mu s)$ width) instrumental response function used for convolution in this mass spectroscopy detection. (b) First-order production rate of 66 000 s⁻¹, utilized for convolution with the response function. (c) Comparison between the convoluted results (brown solid line) and direct kinetic measurement of the m/z = 54product (brown open circles) for [C₃H₆] = 1.43×10^{14} mol/cm³. (d) Kinetic evolution of m/z = 53 (green), 54 (orange), and 55 (violet) products for $[C_3H_6] = 1.43$ × 10¹⁴ mol/cm³. (e) Pseudo-first-order rate of the m/z = 54 product vs C_3H_6 density, along with its linear fit.

observed in the CMB experiment, according to the product translational energy and angular flux distributions. The underlying reaction mechanism will be discussed in Sec. III E. Despite the lack of isomer identification capability in the present work, our results on product detection of the dominant channel at m/z 54 (corresponding to CH + $C_3H_6 \rightarrow C_4H_6 + H)$ qualitatively agree with the previous PIMS and CMB studies, with different C_4H_6 isomers being observed.

The less intense mass peak observed at m/z 53 corresponds to C_4H_5 cations, which have not been detected previously in either PMIS or CMB experiments. One possible explanation for the detection of $C_4H_5^+$ is that it arises from the dissociative ionization

of the energized C_4H_6 primary products. For example, according to the photoionization cross section measurements of 1-butyne (CH₃CH₂CCH), the fragment ion $C_4H_5^+$ appears near 11.04 eV.⁶⁶ If we assume that most of the excess energy (2.37 eV) from the CH + propene exoergic reaction goes into the internal excitation of 1-butyne, and that the cooling effect from the bath gas is negligible (although it is not likely, as the collision frequency is >10⁶ s⁻¹ under the flow conditions), it may be possible to observe $C_4H_5^+$ from dissociative ionization of 1-butyne with our VUV photoionization probe (10.48 eV). Another possible explanation for the observation of $C_4H_5^+$ is that it arises from the CH + $C_3H_6 \rightarrow C_4H_5 + H_2$ reaction channel. Some C_4H_5 radical isomers, along with their ionization

TABLE I. C_4H_6 isomer name, its adiabatic ionization energy, and reaction energy to form the corresponding C_4H_6+H product channel

Species name	Chemical formula	Ionization energy (eV)	Reaction energy (kcal mol ⁻¹) ^a
1,3-butadiene	CH ₂ =CHCH=CH ₂	9.08 ^b	-67.8
1,2-butadiene	$CH_3CH=C=CH_2$	9.23 ^b	-55.8
1-butyne	CH ₃ CH ₂ C≡CH	10.20^{b}	-54.6
2-butyne	CH ₃ C≡CCH ₃	9.59 ^b	-59.7
Cyclobutene	$c(CH_2CH=CHCH_2)$	9.43 ^b	-56.2
Methylenecyclopropane	$CH_2 = c(CCH_2CH_2)$	9.6 ^b	-48.3
1-methylcyclopropene	$CH_3-c(CHCHCH)$	9.12 ^c	-34.2
3-methylcyclopropene	$CH_3-c(C=CHCH_2)$	9.06 ^c	-37.4

^aCalculated results in Ref. 54.

energies and reaction energies associated with C₄H₅ + H₂ reaction channels, are summarized in Table S1. From an energetic point of view, it is feasible to form C₄H₅ + H₂ as a product of the CH + propene reaction, even though this channel has not been predicted theoretically or detected experimentally. The potential energy surface of C₃H₅ radical has been calculated by Narendrapurapu et al.,⁶⁷ with a predicted conversion pathway predicted from C₃H₄ + H (allene + H and propyne + H) to $C_3H_3 + H_2$ (propargyl + H_2). Since C₄H₇ is the methyl derivative of C₃H₅, a similar pathway could exist here, leading to the C₄H₅ + H₂ product channel from the highly exothermic CH + C₃H₆ reaction. A tunable VUV source is again desired to confirm whether the mass peak at m/z 53 arises from dissociative ionization or from a reaction product channel. This will be part of future work when this apparatus is coupled to the Dalian Coherent Light Source, a tunable free electron laser user facility in China that operates in the 50-150 nm region with high pulse energy and a repetition rate up to 50 Hz.

tant, the bimolecular rate coefficient, can also be determined from the time-dependent evolution of the reaction products. The CH + C_3H_6 reaction produces multiple products P_m along with accompanying coproducts Y_m , expressed as CH + $C_3H_6 \stackrel{k_m}{\rightarrow} P_m + Y_m$ with $\sum_m k_m = k_2$ (m = 1, 2, 3, ...), where k_2 is the overall bimolecular reaction rate coefficient as in (E5), and k_m is the reaction rate coefficient for each product channel. Under pseudo-first-order conditions, the formation of product species P_m is given by

In addition, the LIF kinetics measurements on the radical reac-

$$\frac{d[P_m]}{dt} = k_m [CH]_t [C_3H_6]. \tag{E6}$$

Substituting Eq. (E5) into (E6) and solving the differential equation yields the formation of P_m as follows:

$$[P_m]_t = \frac{k_m [C_3 H_6] [CH]_0}{(k_2 [C_3 H_6] + k_{other})} (1 - \exp[-(k_2 [C_3 H_6] + k_{other}) \cdot t])$$

$$= \frac{k_m [C_3 H_6] [CH]_0}{k_{1st}} (1 - \exp[-k_{1st} \cdot t]).$$
 (E7)

Equation (E7) shows that the product evolution $[P_m]_t$ increases exponentially with the pseudo-first-order rate $k_{1st} = k_2[C_3H_6]$ + k_{other} of the overall reaction, and it is important to note that this trend is independent from each product channel. Therefore, we can employ the same method used in LIF measurements to determine the bimolecular reaction rate coefficient k_2 via ReTOFMS by obtaining the slope of the values of k_{1st} vs the reactant concentration [C₃H₆]. Since ReTOFMS has a response function, as discussed in Sec. III C, Eq. (E7) is convoluted with a Gaussian profile with a width of 12 μ s to fit the experimental product evolution (m/z = 54) as shown in Figs. 5(a)-5(c). The resultant pseudo-first-order rate coefficients as a function of reactant density are shown in Fig. 5(e). A bimolecular rate coefficient of $(5.8 \pm 2.9) \times 10^{-10}$ cm³ molecule⁻¹ s⁻¹ for the CH + propene reaction is obtained from the weighted linear fit in Fig. 5(e). The k_2 value obtained from ReTOFMS has a large uncertainty and is almost twice that from the LIF kinetics measurement in Sec. III B. This large uncertainty is due to the low signal level combined with the influence of the velocity spread during transit from the skimmer tip to the photoionization probe region. The overestimated k2 value from ReTOFMS compared to the LIF result may arise from an overestimation of the FWHM of the Gaussian system response function. Nevertheless, our results clearly indicate that the CH + propene reaction produces C₄H₆ + H products. Furthermore, we prefer to report the LIF kinetics results, $k_2 = (3.4 \pm 0.6)$ \times 10⁻¹⁰ cm³ molecule⁻¹ s⁻¹, as the overall rate coefficient of the CH + propene reaction at 23(3) K. This rate coefficient value is smaller than those measured at temperatures from 77 to 298 K, as shown in Fig. 6. The second-order rate coefficients increase as the temperature decreases to 77 K and subsequently drop at 23 K. The similar trend is observed in the reactions between CH and CH₄, methylacetylene, and allene.⁴⁸

E. Reaction mechanism

The CH + propene reaction is barrierless and exothermic, initiated by either CH addition to the double bond in propene or CH insertion into the C–H or C–C bonds of propene. 53,54 The newly formed complex, C_4H_7 , is highly energetic and undergoes further isomerization and decomposition to produce various prod-

^bReference 65.

c Reference 50.

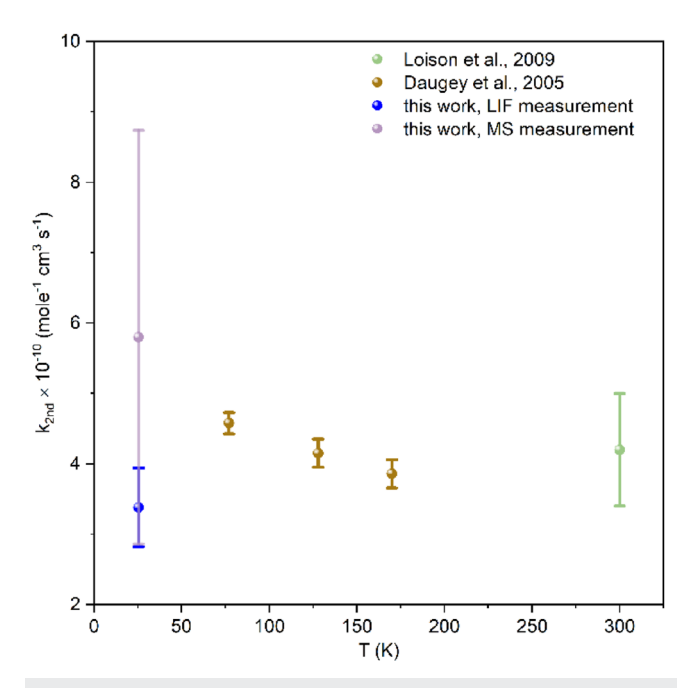


FIG. 6. Comparison of second order reaction rate coefficients for the CH + C_3H_6 reaction at various temperatures and methods. LIF (blue solid circles) and mass spectrometry (violet solid circles) measurements at 23(3) K are presented with $\pm 1\sigma$ error from this work. LIF measurements by Daugey *et al.* using CRESU at 77, 128, and 170 K (brown solid circles) with $\pm 2\sigma$ error.⁴⁸ LIF measurements by Loison *et al.* using a fast-flow reactor at 300 K (green solid circle) are represented with $\pm 1\sigma$ error.⁴⁹

ucts. The reaction product branching ratios (BRs) were calculated both at a zero-pressure limit under single collision conditions and at p = 5 Torr and T = 300 K. The BRs under both conditions appear similar, but they depend on the initial C₄H₇ complex formed in the entrance channel. If the reaction is initiated by CH addition to the double bond in propene or by CH insertion into the terminal sp² C-H bond or the C-C bond, 1,3-butadiene + H is the dominant product (~85%), with a minor (~11%) product channel of ethene + vinyl and a smaller (~4%) channel of 1,2-butadiene + H. If CH inserts into a C-H bond in the terminal CH₃ group, leading to the ·CH2CH2CHCH2 complex, the dominant reaction products are predicted to be ethene + vinyl radical (67%-77%) and 1,3-butadiene + H (20%-30%). If CH inserts into the middle sp^2 C-H bond in propene, $CH_3C(\cdot CH_2)CH_2$ complex is produced, which predominantly decomposes to allene + CH₃ (99%). The computed BRs agree quantitatively well with the experimental results by Loison and Bergeat, who measured the H eliminated product channel, $C_4H_6 + H$, as the dominant channel (BR = 0.78 \pm 0.10) using LIF detection on H atoms in a fast-flow reactor at room temperature.⁴⁹ However, the calculated BRs disagree with the PIMS experiments at p = 4 Torr and T = 298 K by Trevitt et al., who observed only C₄H₆ + H products, with C₄H₆ isomers further identified as 1,3-butadiene (BR = 0.63 ± 0.13), 1,2-butadiene (BR = 0.25 \pm 0.05), and 1-butyne (BR = 0.12 \pm 0.03). In addition, the isotopelabeled CD + propene reaction by Trevitt et al. clearly indicates that the CH addition channel is dominant. This leads to a cyclic C_4H_7 intermediate, which further ring opens to $CH_3CHCH\cdot CH_2$ and decomposes to lose a hydrogen atom, producing 1,3- or 1,2-butadiene. A small amount of 1-butyne (0.12 \pm 0.03) might be formed by secondary H assisted isomerization of 1,2-butadiene. Overall, the statistical Rice–Ramsperger–Kassel–Marcus (RRKM) calculations and the PIMS experimental results indicate that the CH + propene reaction predominantly produces 1,3-butadiene + H.

The dynamics study under single-collision conditions, conducted via a crossed molecular beam experiment, revealed that the cyclic products 1-methylcyclopropene and 3-methylcyclopropene are formed in the CH + propene reaction.⁵¹ This finding clearly contradicts both the experimental kinetics measurements and the theoretical RRKM theory results, which suggest that 1,3-butadiene + H is the major product channel, demonstrating a critical non-RRKM behavior in the reaction. Systematic experimental isotope-labeled reactions, such as CH + CD₃CD=CD₂, CD + CH₃CH=CH₂, and CD + CD₃CHCH₂, further confirmed that this reaction is initiated by CH addition to the double bond in propene, forming a cyclic C₄H₇ intermediate, CH₃c(CHCHCH₂), which is consistent with the PIMS study. However, the experimentally derived reaction energy of -168 ± 25 kJ mol⁻¹ and a tight exit transition state from decomposing long-lived reaction intermediates in CMB suggest that the H atom loss to form 1-methylcyclopropene and 3-methylcyclopropene occurs on a timescale faster than the isomerization of CH₃-c(CH·CHCH₂), a methyl-substituted cyclopropyl radical intermediate. The CMB experiment under single-collision conditions studied the reaction dynamics by observing the nascent product distributions, which provide a glimpse of the reaction products (1-methylcyclopropene and 3-methylcyclopropene). In contrast, under thermal conditions, where more collisions with bath gas occur and the time scale for reaction intermediates to isomerize is longer, the kinetics studies by Trevitt et al. 50 in a flow reactor detected 1,3-butadiene as the major product, as predicted by statistical RRKM calculations. Similarly, we expect 1,3-butadiene to be the dominant product under the present Laval uniform supersonic flow conditions. Since the single VUV wavelength (118.27 nm) used for the photoionization does not permit isomer-specific analysis, a lowtemperature kinetics study station is being developed at the Dalian Coherent Light Source. With a tunable VUV probe and ReTOFMS, this will provide a definitive answer.

F. Astrochemical importance

Both the methylidyne radical (CH $\rm X^2\Pi$) and propene (C₃H₆) have been detected in dark cold molecular clouds (e.g., TMC-1, Lupus-1a, L1495B, L1521F, and Serpens South 1a) and in the low-mass protostar IRAS 16293-2422 B. ^{68–71} The CH radical possesses an unpaired electron and an empty molecular orbital, contributing to its high ground-state reactivity. This reactivity significantly influences hydrocarbon growth and the synthesis of complex organic molecules under low-temperature interstellar conditions. Currently, over 50 interstellar hydrocarbon species have been detected, most of which exhibit a high degree of unsaturation. However, the formation mechanisms of many of these unsaturated hydrocarbons remain poorly understood, highlighting a critical area of research in astrochemistry.

This study demonstrates that the reaction between CH and propene at low temperature forms a complex that proceeds via H elimination, producing unsaturated hydrocarbons such as C₄H₆ isomers. Among these, 1,3-butadiene (a C₄H₆ isomer) has been identified as the primary product at room temperature.⁵⁰ Notably, 1,3-butadiene can further react with ethynyl radicals (C₂H) to form benzene, the simplest PAH molecule under interstellar conditions.⁵⁵ The C₄H₅ isomers, including 1,3-butadien-2-yl, 1-butyn-3-yl, and 2butyn-1-yl radicals, are also highly unsaturated and may contribute to the formation of PAHs and other complex organic species in the interstellar conditions. However, proving this experimentally is challenging due to the difficulty in generating these radicals with high density. The present work highlights the significant role of the CH radical in forming highly unsaturated hydrocarbons, warranting its inclusion in the astrochemical modeling in the dark cold molecular clouds. Incorporating CH driven reactions into astrochemical models may improve predictions of unsaturated hydrocarbon and PAH abundances, refining our understanding of molecular complexity in the early stages of star and planet formation.

IV. CONCLUSION

We have developed a new instrument for studying the reaction kinetics and dynamics of astrochemically important reactions at low temperatures. In this setup, two well-established detection techniques, LIF and VUV photoionization ReTOFMS, have been successfully coupled to a supersonic uniform low-temperature flow. A helium Laval nozzle designed with a Mach number of 6 was characterized, achieving a temperature of 23 ± 3 K and a density of $(2.0 \pm 0.4) \times 10^{16}$ molecule cm⁻³. The second-order rate coefficient for the reaction between the methylidyne radical (CH) and propene (C₃H₆) is measured at 23(3) K using LIF, yielding $k_2 = (3.4 \pm 0.6) \times 10^{-10} \text{ cm}^3 \text{ molecule}^{-1} \text{ s}^{-1}$. VUV (118.27 nm) photoionization ReTOFMS detected a dominant product channel, CH $+ C_3H_6 \rightarrow C_4H_6 + H$, without isomer identification. Another less intense mass peak at m/z 53 was also observed, which could either result from the dissociative ionization of the energized C₄H₆ primary products or indicate another product channel, C₄H₅ + H₂. Given that both CH and C₃H₆ are present in cold molecular clouds (e.g., TMC-1, Lupus-1a, L1495B, L1521F, and Serpens South 1a), these products, particularly the (isomeric) C₄H₆ species, are likely to exist in interstellar environments. Their contribution to the formation of highly unsaturated hydrocarbons should be considered in astrochemical models of cold molecular clouds to improve predictions of unsaturated hydrocarbon and PAH abundances, advancing our understanding of molecular complexity in early star and planet formation.

SUPPLEMENTARY MATERIAL

The supplementary material contains more information on the linear correlation of MS and propene density in the flow, a comparison of the gas profile from Pitot and MS measurements, an analysis of the instrument response function, and selected C₄H₅ isomer information.

ACKNOWLEDGMENTS

The authors gratefully acknowledge the Dalian Coherent Light Source (DCLS) for support and assistance. This work was supported by the National Natural Science Foundation of China

(Grant No. 22273103), the National Natural Science Foundation of China (NSFC Center for Chemical Dynamics) (Grant No. 22288201), Dalian Institute of Chemical Physics (Grant No. DICP I202230), and the Scientific Instrument Developing Project of the Chinese Academy of Sciences (Grant No. GJJSTD20220001).

AUTHOR DECLARATIONS

Conflict of Interest

The authors have no conflicts to disclose.

Author Contributions

F.Z. and S.M. contributed equally to this work.

Feiyue Zhou: Data curation (equal); Formal analysis (equal); Methodology (equal); Resources (equal); Validation (equal); Writing - original draft (equal); Writing - review & editing (equal). Shuze Ma: Data curation (equal); Formal analysis (equal); Methodology (equal); Resources (equal); Validation (equal); Writing original draft (equal); Writing - review & editing (equal). Lei Li: Data curation (supporting); Formal analysis (supporting); Methodology (supporting); Resources (equal); Validation (equal); Writing – original draft (supporting); Writing - review & editing (supporting). Jiale Zhang: Data curation (supporting); Formal analysis (supporting); Methodology (supporting); Resources (equal); Validation (equal); Writing - original draft (supporting); Writing - review & editing (supporting). Chunlei Xiao: Data curation (supporting); Formal analysis (supporting); Investigation (supporting); Methodology (supporting); Project administration (supporting); Resources (equal); Supervision (supporting); Validation (equal); Writing original draft (supporting); Writing - review & editing (supporting). Wenrui Dong: Funding acquisition (supporting); Investigation (supporting); Methodology (supporting); Project administration (supporting); Supervision (supporting); Validation (supporting); Writing - review & editing (supporting). Hongwei Li: Conceptualization (lead); Data curation (supporting); Formal analysis (supporting); Funding acquisition (lead); Investigation (equal); Methodology (equal); Supervision (equal); Writing - original draft (equal); Writing - review & editing (equal).

DATA AVAILABILITY

The data that support the findings of this study are available within the article and its supplementary material. If additional data are required, please contact the corresponding author.

REFERENCES

- ¹C. P. Endres, S. Schlemmer, P. Schilke, J. Stutzki, and H. S. P. Müller, "The cologne database for molecular spectroscopy, CDMS, in the virtual atomic and molecular data centre, VAMDC," J. Mol. Spectrosc. 327, 95-104 (2016).
- ²B. A. McGuire, "2021 census of interstellar, circumstellar, extragalactic, protoplanetary disk, and exoplanetary molecules," Astrophys. J., Suppl. Ser. 259, 30
- ³ A. Leger and J. L. Puget, "Identification of the 'unidentified' IR emission features of interstellar dust?," Astron. Astrophys. 137, L5-L8 (1984), https://ui.adsabs.harvard.edu/abs/1984A&A...137L...5L.

- ⁴L. J. Allamandola, A. G. G. M. Tielens, and J. R. Barker, "Polycyclic aromatic hydrocarbons and the unidentified infrared emission bands: Auto exhaust along the Milky Way," Astrophys. J. **290**, L25–L28 (1985).
- ⁵T. J. Millar, C. Walsh, M. Van de Sande, and A. J. Markwick, "The UMIST database for astrochemistry 2022," Astron. Astrophys. **682**, A109 (2024).
- ⁶ V. Wakelam, J. C. Loison, E. Herbst, B. Pavone, A. Bergeat, K. Béroff, M. Chabot, A. Faure, D. Galli, W. D. Geppert, D. Gerlich, P. Gratier, N. Harada, K. M. Hickson, P. Honvault, S. J. Klippenstein, S. D. L. Picard, G. Nyman, M. Ruaud, S. Schlemmer, I. R. Sims, D. Talbi, J. Tennyson, and R. Wester, "The 2014 KIDA network for interstellar chemistry," Astrophys. J., Suppl. Ser. 217, 20 (2015).
- ⁷S.-M. Tsai, J. R. Lyons, L. Grosheintz, P. B. Rimmer, D. Kitzmann, and K. Heng, "VULCAN: An open-source, validated chemical kinetics Python code for exoplanetary atmospheres," Astrophys. J., Suppl. Ser. 228, 20 (2017).
- ⁸M. Dobrijevic, J. C. Loison, V. Hue, T. Cavalié, and K. M. Hickson, "1D photochemical model of the ionosphere and the stratosphere of Neptune," Icarus 335, 113375 (2020).
- ⁹J. M. Mendonça, S.-m. Tsai, M. Malik, S. L. Grimm, and K. Heng, "Three-dimensional circulation driving chemical disequilibrium in WASP-43b," Astrophys. J. **869**, 107 (2018).
- ¹⁰R. J. Shannon, M. A. Blitz, A. Goddard, and D. E. Heard, "Accelerated chemistry in the reaction between the hydroxyl radical and methanol at interstellar temperatures facilitated by tunnelling," Nat. Chem. 5, 745–749 (2013).
- 11 M. Tizniti, S. D. Le Picard, F. Lique, C. Berteloite, A. Canosa, M. H. Alexander, and I. R. Sims, "The rate of the F + $\rm H_2$ reaction at very low temperatures," Nat. Chem. 6, 141–145 (2014).
- 12 S. Blázquez, D. González, A. García-Sáez, M. Antiñolo, A. Bergeat, F. Caralp, R. Mereau, A. Canosa, B. Ballesteros, J. Albaladejo, and E. Jiménez, "Experimental and theoretical investigation on the OH + CH₃C(O)CH₃ reaction at interstellar temperatures (T = 11.7–64.4 K)," ACS Earth Space Chem. 3, 1873–1883 (2019).
- 13 D. Nuñez-Reyes, K. M. Hickson, J.-C. Loison, R. F. K. Spada, R. M. Vichietti, F. B. C. Machado, and R. L. A. Haiduke, "Tunneling enhancement of the gas-phase CH + CO₂ reaction at low temperature," J. Phys. Chem. A **124**, 10717–10725 (2020).
- ¹⁴C. Berteloite, M. Lara, A. Bergeat, S. D. Le Picard, F. Dayou, K. M. Hickson, A. Canosa, C. Naulin, J.-M. Launay, I. R. Sims, and M. Costes, "Kinetics and dynamics of the $S(^1D) + H_2 \rightarrow SH + H$ reaction at very low temperatures and collision energies," Phys. Rev. Lett. **105**, 203201 (2010).
- ¹⁵D. Gupta, S. Cheikh Sid Ely, I. R. Cooke, T. Guillaume, O. Abdelkader Khedaoui, T. S. Hearne, B. M. Hays, and I. R. Sims, "Low temperature kinetics of the reaction between methanol and the CN radical," J. Phys. Chem. A 123, 9995–10003 (2019).
- 16 B. R. Rowe, G. Dupeyrat, J. B. Marquette, and P. Gaucherel, "Study of the reactions $N_2{}^+ + 2N_2 \rightarrow N_4{}^+ + N_2$ and $O_2{}^+ + 2O_2 \rightarrow O_4{}^+ + O_2$ from 20 to 160 K by the CRESU technique," J. Chem. Phys. **80**, 4915–4921 (1984).
- $^{17}\text{B. R. Rowe, G. Dupeyrat, J. B. Marquette, D. Smith, N. G. Adams, and E. E. Ferguson, "The reaction <math display="inline">{\rm O_2}^+ + {\rm CH_4} \rightarrow {\rm CH_3O_2}^+ + {\rm H}$ studied from 20 to 560 K in a supersonic jet and in a SIFT," J. Chem. Phys. **80**, 241–245 (1984).
- ¹⁸B. R. Rowe, J. B. Marquette, and C. Rebrion, "Mass-selected ion-molecule reactions at very low-temperatures. The CRESUS apparatus," J. Chem. Soc., Faraday Trans. 2 **85**, 1631–1641 (1989).
- ¹⁹B. Joalland, N. Jamal-Eddine, D. Papanastasiou, A. Lekkas, S. Carles, and L. Biennier, "A mass-selective ion transfer line coupled with a uniform supersonic flow for studying ion-molecule reactions at low temperatures," J. Chem. Phys. 150, 164201 (2019).
- ²⁰S. E. Taylor, A. Goddard, M. A. Blitz, P. A. Cleary, and D. E. Heard, "Pulsed Laval nozzle study of the kinetics of OH with unsaturated hydrocarbons at very low temperatures," Phys. Chem. Chem. Phys. 10, 422–437 (2008).
- ²¹ J. Daranlot, M. Jorfi, C. J. Xie, A. Bergeat, M. Costes, P. Caubet, D. Q. Xie, H. Guo, P. Honvault, and K. M. Hickson, "Revealing atom-radical reactivity at low temperature through the N + OH reaction," Science 334, 1538–1541 (2011).
- ²²D. E. Heard, "Rapid acceleration of hydrogen atom abstraction reactions of OH at very low temperatures through weakly bound complexes and tunneling," Acc. Chem. Res. 51, 2620–2627 (2018).
- $^{\bf 23}$ K. M. Hickson, P. Caubet, and J. C. Loison, "Unusual low-temperature reactivity of water: The CH + $\rm H_2O$ reaction as a source of interstellar formaldehyde?," J. Phys. Chem. Lett. 4, 2843–2846 (2013).

- ²⁴A. Canosa, I. R. Sims, D. Travers, I. W. M. Smith, and B. R. Rowe, "Reactions of the methylidine radical with CH₄, C₂H₂, C₂H₄, C₂H₆, and but-1-ene studid between 23 and 295 K with a CRESU apparatus," Astron. Astrophys. **323**, 644–651 (1997), https://ui.adsabs.harvard.edu/abs/1997A&A...323..644C.
- ²⁵ K. M. Douglas, D. I. Lucas, C. Walsh, N. A. West, M. A. Blitz, and D. E. Heard, "The gas-phase reaction of NH₂ with formaldehyde (CH₂O) is not a source of formamide (NH₂CHO) in interstellar environments," Astrophys. J., Lett. **937**, L16 (2022).
- $^{\mathbf{26}}$ D. Chastaing, P. L. James, I. R. Sims, and I. W. M. Smith, "Neutral–neutral reactions at the temperatures of interstellar clouds: Rate coefficients for reactions of atomic carbon, $C(^3P)$, with O_2, C_2H_2, C_2H_4 and C_3H_6 down to 15 K," Phys. Chem. Chem. Phys. 1, 2247–2256 (1999).
- $^{\bf 27}$ A. Bergeat, K. M. Hickson, N. Daugey, P. Caubet, and M. Costes, "A low temperature investigation of the N(4 S°) + NO reaction," Phys. Chem. Chem. Phys. 11, 8149–8155 (2009).
- ²⁸ K. M. Hickson, A. Bergeat, and M. Costes, "A low temperature study of the reactions of atomic chlorine with simple alkanes," J. Phys. Chem. A 114, 3038–3044 (2010).
- ²⁹C. Abeysekera, L. N. Zack, G. B. Park, B. Joalland, J. M. Oldham, K. Prozument, N. M. Ariyasingha, I. R. Sims, R. W. Field, and A. G. Suits, "A chirped-pulse Fourier-transform microwave/pulsed uniform flow spectrometer. II. Performance and applications for reaction dynamics," J. Chem. Phys. 141, 214203 (2014).
- ³⁰ J. M. Oldham, C. Abeysekera, B. Joalland, L. N. Zack, K. Prozument, I. R. Sims, G. B. Park, R. W. Field, and A. G. Suits, "A chirped-pulse Fourier-transform microwave/pulsed uniform flow spectrometer. I. The low-temperature flow system," J. Chem. Phys. 141, 154202 (2014).
- ³¹T. Guillaume, B. M. Hays, D. Gupta, I. R. Cooke, O. Abdelkader Khedaoui, T. S. Hearne, M. Drissi, and I. R. Sims, "Product-specific reaction kinetics in continuous uniform supersonic flows probed by chirped-pulse microwave spectroscopy," J. Chem. Phys. 160, 204201 (2024).
- ³² R. M. Gurusinghe, N. Dias, R. Krueger, and A. G. Suits, "Uniform supersonic flow sampling for detection by chirped-pulse rotational spectroscopy," J. Chem. Phys. 156, 014202 (2022).
- ³³S. Thawoos, N. Suas-David, R. M. Gurusinghe, M. Edlin, A. Behzadfar, J. X. Lang, and A. G. Suits, "Low temperature reaction kinetics inside an extended Laval nozzle: REMPI characterization and detection by broadband rotational spectroscopy," J. Chem. Phys. 159, 214201 (2023).
- ³⁴N. Suas-David, S. Thawoos, and A. G. Suits, "A uniform flow-cavity ring-down spectrometer (UF-CRDS): A new setup for spectroscopy and kinetics at low temperature," J. Chem. Phys. 151, 244202 (2019).
- ³⁵M. Louviot, N. Suas-David, V. Boudon, R. Georges, M. Rey, and S. Kassi, "Strong thermal nonequilibrium in hypersonic CO and CH₄ probed by CRDS," J. Chem. Phys. **142**, 214305 (2015).
- ³⁶M. Lippe, U. Szczepaniak, G. L. Hou, S. Chakrabarty, J. J. Ferreiro, E. Chasovskikh, and R. Signorell, "Infrared spectroscopy and mass spectrometry of CO₂ clusters during nucleation and growth," J. Phys. Chem. A **123**, 2426–2437 (2019).
- ³⁷D. I. Lucas, T. Guillaume, D. E. Heard, and J. H. Lehman, "Design and implementation of a new apparatus for astrochemistry: Kinetic measurements of the CH + OCS reaction and frequency comb spectroscopy in a cold uniform supersonic flow," J. Chem. Phys. 161, 094203 (2024).
- ³⁸S. Lee, R. J. Hoobler, and S. R. Leone, "A pulsed Laval nozzle apparatus with laser ionization mass spectroscopy for direct measurements of rate coefficients at low temperatures with condensable gases," Rev. Sci. Instrum. 71, 1816–1823 (2000).
- 39 S. Lee and S. R. Leone, "Rate coefficients for the reaction of C_2 H with O_2 at 90 K and 120 K using a pulsed Laval nozzle apparatus," Chem. Phys. Lett. **329**, 443–449 (2000)
- 40 S. Lee, D. A. Samuels, R. J. Hoobler, and S. R. Leone, "Direct measurements of rate coefficients for the reaction of ethynyl radical (C_2 H) with C_2 H₂ at 90 and 120 K using a pulsed Laval nozzle apparatus," J. Geophys. Res.: Planets 105, 15085–15090, https://doi.org/10.1029/1999je001187 (2000).
- ⁴¹B. Schläppi, J. H. Litman, J. J. Ferreiro, D. Stapfer, and R. Signorell, "A pulsed uniform Laval expansion coupled with single photon ionization and mass spectrometric detection for the study of large molecular aggregates," Phys. Chem. Chem. Phys. 17, 25761–25771 (2015).

- ⁴²J. Krohn, M. Lippe, C. X. Li, and R. Signorell, "Carbon dioxide and propane nucleation: The emergence of a nucleation barrier," Phys. Chem. Chem. Phys. 22, 15986–15998 (2020).
- ⁴³H. Sabbah, L. Biennier, S. J. Klippenstein, I. R. Sims, and B. R. Rowe, "Exploring the role of PAHs in the formation of soot: Pyrene dimerization," J. Phys. Chem. Lett. 1, 2962–2967 (2010).
- ⁴⁴S. Soorkia, C.-L. Liu, J. D. Savee, S. J. Ferrell, S. R. Leone, and K. R. Wilson, "Airfoil sampling of a pulsed Laval beam with tunable vacuum ultraviolet synchrotron ionization quadrupole mass spectrometry: Application to low-temperature kinetics and product detection," Rev. Sci. Instrum. **82**, 124102 (2011).
- ⁴⁵O. Durif, M. Capron, J. P. Messinger, A. Benidar, L. Biennier, J. Bourgalais, A. Canosa, J. Courbe, G. A. Garcia, J. F. Gil, L. Nahon, M. Okumura, L. Rutkowski, I. R. Sims, J. Thiévin, and S. D. Le Picard, "A new instrument for kinetics and branching ratio studies of gas phase collisional processes at very low temperatures," Rev. Sci. Instrum. 92, 014102 (2021).
- 46 J. Bouwman, F. Goulay, S. R. Leone, and K. R. Wilson, "Bimolecular rate constant and product branching ratio measurements for the reaction of C_2H with ethene and propene at 79 K," J. Phys. Chem. A 116, 3907–3917 (2012).
- ⁴⁷J. Bouwman, M. Fournier, I. R. Sims, S. R. Leone, and K. R. Wilson, "Reaction rate and isomer-specific product branching ratios of $C_2H + C_4H_8$: 1-butene, *cis*-2-butene, *trans*-2-butene, and isobutene at 79 K," J. Phys. Chem. A **117**, 5093–5105 (2013).
- ⁴⁸N. Daugey, P. Caubet, B. Retail, M. Costes, A. Bergeat, and G. Dorthe, "Kinetic measurements on methylidyne radical reactions with several hydrocarbons at low temperatures," Phys. Chem. Chem. Phys. 7, 2921–2927 (2005).
- 49 J. C. Loison and A. Bergeat, "Rate constants and the H atom branching ratio of the reactions of the methylidyne CH(X 2 II) radical with C₂H₂, C₂H₄, C₃H₄ (methylacetylene and allene), C₃H₆ (propene) and C₄H₈ (*trans*-butene)," Phys. Chem. Chem. Phys. 11, 655–664 (2009).
- ⁵⁰ A. J. Trevitt, M. B. Prendergast, F. Goulay, J. D. Savee, D. L. Osborn, C. A. Taatjes, and S. R. Leone, "Product branching fractions of the CH + propene reaction from synchrotron photoionization mass spectrometry," J. Phys. Chem. A 117, 6450–6457 (2013).
- ⁵¹ C. He, A. M. Thomas, G. R. Galimova, A. M. Mebel, and R. I. Kaiser, "Gas-phase formation of 1-methylcyclopropene and 3-methylcyclopropene via the reaction of the methylidyne radical (CH; $X^2\Pi$) with propylene (CH₃CHCH₂; X^1A')," J. Phys. Chem. A **123**, 10543–10555 (2019).
- 52 J. L. Miller, "Theoretical study of the straight-chain C_4H_7 radical isomers and their dissociation and isomerization transition states," J. Phys. Chem. A $108,\,2268-2277\,(2004).$
- ⁵³Y. Li, H. L. Liu, Z. J. Zhou, X. R. Huang, and C. C. Sun, "Reaction mechanism of CH + C₃H₆: A theoretical study," J. Phys. Chem. A **114**, 9496–9506 (2010).
- 54 J. M. Ribeiro and A. M. Mebel, "Reaction mechanism and product branching ratios of the CH + C_3H_6 reaction: A theoretical study," J. Phys. Chem. A 120, 1800–1812 (2016).
- ⁵⁵B. M. Jones, F. Zhang, R. I. Kaiser, A. Jamal, A. M. Mebel, M. A. Cordiner, and S. B. Charnley, "Formation of benzene in the interstellar medium," Proc. Natl. Acad. Sci. U. S. A. 108, 452–457 (2011).
- ⁵⁶C. Romanzin, S. Boyé-Péronne, D. Gauyacq, Y. Bénilan, M. C. Gazeau, and S. Douin, "CH radical production from 248 nm photolysis or discharge-jet

- dissociation of CHBr₃ probed by cavity ring-down absorption spectroscopy," J. Chem. Phys. **125**, 114312 (2006).
- ⁵⁷D. B. Atkinson and M. A. Smith, "Design and characterization of pulsed uniform supersonic expansions for chemical applications," Rev. Sci. Instrum. 66, 4434–4446 (1995).
- 58 G. Dupeyrat, J. B. Marquette, and B. R. Rowe, "Design and testing of axisymmetric nozzles for ion-molecule reaction studies between 20 $^{\circ}$ K and 160 $^{\circ}$ K," Phys. Fluids 28, 1273–1279 (1985).
- 59 S. Ma, F. Zhou, G. Sun, C. Xiao, W. Dong, H. Li, and X. Yang, "Collision-induced relaxation of CH(X $^2\Pi$, v = 0) radical by He, Ar, and N $_2$ under low-temperature supersonic flow condition," Chin. J. Chem. Phys. (to be published) (2024).
- ⁶⁰C. M. Western and B. E. Billinghurst, "Automatic and semi-automatic assignment and fitting of spectra with PGOPHER," Phys. Chem. Chem. Phys. 21, 13986–13999 (2019).
- ⁶¹ R. Kepa, A. Para, M. Rytel, and M. Zachwieja, "New spectroscopic analysis of the $B^2\Sigma^--X^2\Pi$ band system of the CH molecule," J. Mol. Spectrosc. **178**, 189–193 (1996).
- 62 G. N. A. Vanveen, T. Baller, A. E. Devries, and N. J. A. Vanveen, "The excitation of the umbrella mode of CH₃ and CD₃ formed from photodissociation of CH₃I and CD₃I at 248 nm," Chem. Phys. **87**, 405–417 (1984).
- ⁶³ R. de Nalda, J. Durá, A. García-Vela, J. G. Izquierdo, J. González-Vázquez, and L. Bañares, "A detailed experimental and theoretical study of the femtosecond Aband photodissociation of CH₃I," J. Chem. Phys. 128, 244309 (2008).
- ⁶⁴C. A. Taatjes, "How does the molecular velocity distribution affect kinetics measurements by time-resolved mass spectrometry?," Int. J. Chem. Kinet. **39**, 565–570 (2007).
- ⁶⁵P. J. Linstrom and W. G. Mallard, NIST Chemistry WebBook, NIST Standard Reference Database Number 69 (National Institute of Standards and Technology, Gaithersburg, MD, 2024).
- ⁶⁶ J. Wang, B. Yang, T. A. Cool, N. Hansen, and T. Kasper, "Near-threshold absolute photoionization cross-sections of some reaction intermediates in combustion," Int. J. Mass Spectrom. 269, 210–220 (2008).
- 67 B. S. Narendrapurapu, A. C. Simmonett, H. F. Schaefer, J. A. Miller, and S. J. Klippenstein, "Combustion chemistry: Important features of the C_3H_5 potential energy surface, including allyl radical, propargyl + H_2 , allene + H, and eight transition states," J. Phys. Chem. A 115, 14209-14214 (2011).
- ⁶⁸S. Manigand, A. Coutens, J. C. Loison, V. Wakelam, H. Calcutt, H. S. P. Müller, J. K. Jørgensen, V. Taquet, S. F. Wampfler, T. L. Bourke, B. M. Kulterer, E. F. van Dishoeck, M. N. Drozdovskaya, and N. F. W. Ligterink, "The ALMA-PILS survey: First detection of the unsaturated 3-carbon molecules propenal (C₂H₃CHO) and propylene (C₃H₆) towards IRAS 16293-2422 B," Astron. Astrophys. 645, A53 (2021)
- ⁶⁹N. Marcelino, J. Cernicharo, M. Agúndez, E. Roueff, M. Gerin, J. Martín-Pintado, R. Mauersberger, and C. Thum, "Discovery of interstellar propylene (CH₃CHCH₂): Missing links in interstellar gas-phase chemistry," Astrophys. J. **665**. L127–L130 (2007).
- ⁷⁰M. Agúndez, J. Cernicharo, and M. Guélin, "Discovery of interstellar ketenyl (HCCO), a surprisingly abundant radical," Astron. Astrophys. 577, L5 (2015).
- ⁷¹ A. Suutarinen, W. D. Geppert, J. Harju, A. Heikkilä, S. Hotzel, M. Juvela, T. J. Millar, C. Walsh, and J. G. A. Wouterloot, "CH abundance gradient in TMC-1," Astron. Astrophys. 531, A121 (2011).